Centrality metric for the vulnerability of urban networks to toxic releases

Centrality metric for the vulnerability of urban networks to toxic releases

Sofia Fellini*
Department of Environmental, Land and Infrastructure Engineering, Politecnico di Torino, 10129 Turin, Italy and Laboratoire de Mécanique des Fluides et d'Acoustique, UMR CNRS 5509, Université de Lyon, École Centrale de Lyon, INSA Lyon, Université Claude Bernard Lyon I, 69134 Écully, France

Pietro Salizzoni
Laboratoire de Mécanique des Fluides et d'Acoustique, UMR CNRS 5509, Université de Lyon, École Centrale de Lyon, INSA Lyon, Université Claude Bernard Lyon I, 69134 Écully, France

Luca Ridolfi
Department of Environmental, Land and Infrastructure Engineering, Politecnico di Torino, 10129 Turin, Italy

(Received 15 December 2019; accepted 2 March 2020; published 31 March 2020)

The dispersion of airborne pollutants in the urban atmosphere is a complex, canopy-driven process. The intricate structure of the city, the high number of potential sources, and the large spatial domain make it difficult to predict dispersion patterns, to simulate a great number of scenarios, and to identify the high-impact emission areas. Here we show that these complex transport dynamics can be efficiently characterized by adopting a complex network approach. The urban canopy layer is represented as a complex network. Street canyons and their intersections shape the spatial structure of the network. The direction and the transport capacity of the flow in the streets define the direction and the weight of the links. Within this perspective, pollutant contamination from a source is modeled as a spreading process on a network, and the most dangerous areas in a city are identified as the best spreading nodes. To this aim, we derive a centrality metric tailored to mass transport in flow networks. By means of the proposed approach, vulnerability maps of cities are rapidly depicted, revealing the nontrivial relation between urban topology, transport capacity of the street canyons, and forcing of the external wind. The network formalism provides promising insight in the comprehensive analysis of the fragility of cities to air pollution.

DOI: 10.1103/PhysRevE.101.032312

I. INTRODUCTION

Cities are extremely vulnerable to air pollution due to the presence of many potential sources and the high population density [1]. Air contamination in urban areas is mainly associated with vehicular traffic, industries, and the heating of buildings. However, terrorist attacks aimed at dispersing toxic gases in crowded spaces (such as city centers) are also feared today [2]. For the development of sustainable and safe cities, public authorities are thus looking for operational tools able to rapidly predict the dispersion of airborne pollutants within the urban canopy. To this aim, computational fluid dynamics and simplified models based on empirical parametrizations have been widely proposed in the last decades. These works evidenced that pollutant transport in the urban atmosphere is strongly driven by the layout of buildings and thus by the street topology of the city (e.g., Refs. [3–6]).

Over the last decade, complex network approaches have demonstrated their great potential in the study of complex systems in multiple domains, from physical (e.g., Refs. [7,8]) to social areas (e.g., Refs. [9]). Recently, a network-based perspective has been proposed for the analysis of fluid-flows systems as wind flows [10], ocean transport [11], and turbulence [12]. By means of a network representation, the structural and dynamical properties of these real-world systems were efficiently characterized. Concerning urban air pollution, we made a first attempt in introducing a complex-network perspective for the identification of the most critical areas for gaseous release in a city [13]. Despite the innovative approach, the lack of adequate formalism limited the use of many concepts and tools (e.g., Refs. [14,15]) developed in the field of complex network theory.

In order to fill this gap, in the present study we provide a formal foundation for modeling pollutant dispersion in the urban atmosphere as a spreading process on a network (e.g., Refs. [16,17]). To this aim, the urban canopy layer is modeled as a weighted and directed complex network. As in Ref. [13], the streets and the street intersections are the links, and the nodes of the network, and the links are oriented according to the wind direction. A fluid dynamic weight is defined to account for the mass transport dynamics along a street canyon and a centrality metric is developed for the detection of the best spreader nodes. In fact, while the identification of best spreader nodes is a well-known classical problem in social, information and technology networks (e.g., Refs. [18–20]), the uncritical application of traditional metrics to mass transport in a flow network reveals some drawbacks. Specifically,

*sofia.fellini@polito.it

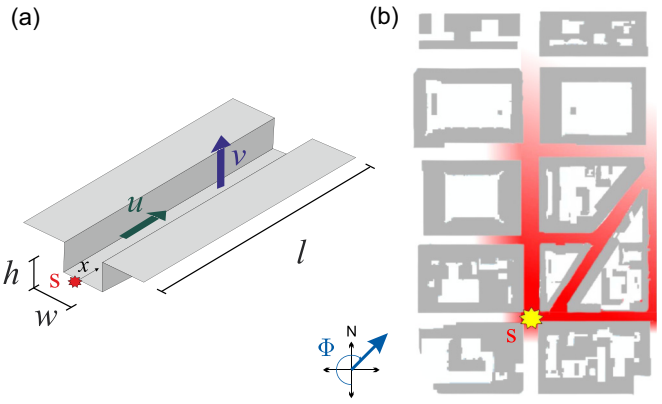

FIG. 1. (a) Representation of a street canyon with the main geometrical and fluid dynamical parameters. (b) Toxic source s within a network of streets. Propagation is mainly driven by the wind approaching the urban canopy with direction Φ, defined as a clockwise angle that is equal to zero for a wind blowing from the north to the south.

the mass conservation of the dispersed substance, the spatial constraints of the physical network, and the nonprobabilistic nature of the contagion (meant as probability of infection between two linked nodes; e.g., Ref. [21]) make this problem original and provide evidence for the need for a tailored centrality metric. Finally, the potential of the proposed approach is assessed by the construction of vulnerability maps of urban districts and by comparison of its performance with that of a more detailed propagation model.

II. PHYSICAL PROBLEM

We consider a high-density urban canopy, made up of street canyons, i.e., narrow streets flanked by high buildings on both sides. This is the typical urban pattern for the city center of most European cities [22]. Within this urban geometry, we focus on an emission scenario with a point source releasing an inert gas at the beginning of a street [Fig. 1(a)]. The dominant transport mechanisms for the passive scalar are (1) the longitudinal transport along the street, (2) the vertical exchange with the atmosphere aloft, and (3) the transport through street intersections. Neglecting longitudinal turbulent diffusion and reentrainment from the atmosphere at the canyon top (see Ref. [13] for details of the physical assumptions), the transport along the street canyon can be modeled as

$$\frac{\partial c}{\partial t} + u\frac{\partial c}{\partial x} + \frac{v}{h}c = 0, \tag{1}$$

where $c(t, x)$ is pollutant concentration as a function of time t and longitudinal distance x, h is the characteristic depth of the street canyon, u is the advective wind velocity along the street, and v is the vertical bulk velocity modeling the turbulent mass transfer between the canyon and the atmosphere. According to the relations proposed by Refs. [23,24], these two velocities are estimated as a function of the external wind intensity and direction (Φ), the geometry of the street canyon, and the aerodynamic roughness of building walls. For both an instantaneous and a continuous release at the source, Eq. (1) gives a concentration at the end of the street [13]

$$c(l/u, l) = c_0 e^{-\frac{l}{u}\frac{v}{h}}, \tag{2}$$

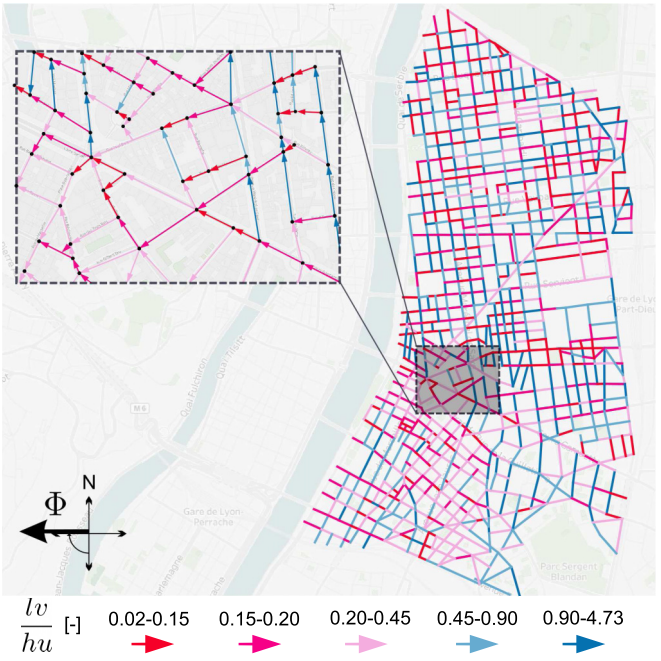

FIG. 2. Network model of a district in Lyon for $\Phi = 90°$. For each link, the color (grayscale intensity) is a function of the exponent of the weight defined in Eq. (3).

where c_0 is the source concentration and l is the street length. Notice that, since both u and v are assumed to be proportional to the friction velocity u_* of the boundary layer flow, Eq. (2) is independent of the intensity of the external wind. In street intersections, complex flow and dispersion patterns take place [25]. As explained in Ref. [13], we adopt a conservative approach, and the pollution front is assumed to propagate towards the streets downwind of the intersection, keeping its concentration unaltered in the crossing.

According to these propagation laws, the gas emitted at the point source spreads through the urban canopy driven by the direction of the external wind Φ, while undergoing an exponential decay in concentration with distance from the source. Introducing a concentration threshold c_{th}, the zone of influence of the source is delimited as the street domain characterized by concentration $c \geqslant c_{\text{th}}$ [shaded streets in Fig. 1(b)]. Under the assumption of uniform residential density, the total length of the streets in the zone of influence is a good index for the danger associated with the source, as it accounts for the number of people affected by the gas release.

III. NETWORK APPROACH

To assess spatial vulnerability of an urban agglomeration, we should reiterate the propagation process for each potential source location, also considering different meteorological scenarios. Given the extent of the urban domain and the nontrivial interconnection between streets, the problem is solved more efficiently by adopting a network-based approach. To this aim, the whole spatially embedded transport domain is modeled as a directed and weighted network $\mathcal{G}(\mathcal{V}, \mathcal{E}, W)$, with node set $\mathcal{V}$, edge set $\mathcal{E}$, and weight matrix W. Network structure (Fig. 2) is given by abstracting street canyons as links and street

intersections as nodes [26]. Link direction is given by the orientation of the longitudinal wind along the street, while link weight reflects the transport capacity of the street canyon. Within this representation, the definition of the weight is crucial as it is the only expression for the physical propagation law. As common in space [27] and flow [28] networks, links are seen here as distances between nodes, i.e. as leak terms for the transport process. Thus, referring to Eq. (2), we define the weight w_{ij} as the cost associated with traversing the link $(i, j) \in \mathcal{E}$, i.e., as the concentration decay along the corresponding street canyon:

$$w_{ij} = e^{\frac{l_{ij} v_{ij}}{u_{ij} h_{ij}}}. \tag{3}$$

In a spreading perspective, the exponent in Eq. (3) can be interpreted as the effective distance between nodes [29]. This distance increases with the average time necessary for the pollution front to propagate longitudinally along the street canyon (l_{ij}/u_{ij}), while it decreases with the average time of vertical transfer of pollutants from the street to the external atmosphere (h_{ij}/v_{ij}).

IV. CENTRALITY METRIC

Given this network representation, the most dangerous locations for the release of airborne pollutants in a city are the best spreader nodes in a complex network. Many metrics are available in literature [19,20,30–34] to detect influential spreaders in SIR-like [35,36] epidemics, e.g., the spreading of infectious diseases in a population or information dissemination in a social environment. These epidemic processes have a stochastic nature since the spreading from one node to another occurs with probability p. Moreover, there is no decay of the spreading potential with distance from the source. On the contrary, the propagation of airborne pollutants is here modeled as a deterministic (i.e., contagion certainly takes place if two links are connected), mass-conservative, and spatial transport process. Thus, the metrics proposed so far are not suitable, and a tailored centrality index for fluid-dynamic spreading potential has to be sought.

Given the physics of the process, we focus on distance-based centralities [37], like closeness and betweenness, since the smaller the distance separating the source node from the other nodes in the network, the greater the toxic concentration that will reach them. While betweenness [38] captures nodes acting as bridges or bottlenecks in network flows [39], closeness centrality [40] is better suited for the identification of best spreader nodes. The closeness centrality of a node s is defined as $C_{\mathrm{clos},s} = 1/\sum_{r\in\mathcal{V}} d_{sr}$, where d_{sr} is the length of the shortest path $\mathcal{D}$ between node s and a generic node r in the network, i.e., the path connecting the two nodes with the minimum number of edges [41]. For a weighted graph, $\mathcal{D}$ is the path that minimizes the sum of the weights of the traversed edges, and thus its length reads

$$d_{sr} = |\mathcal{D}| = \min_{\mathcal{P}} \left(\sum_{(i,j)\in\mathcal{P}} w_{ij} \right) \quad \text{where } \mathcal{P} \text{ is the path from } s \text{ to } r. \tag{4}$$

In our perspective, given Eqs. (3) and (4), $\mathcal{D}$ is the critical propagation path between the two nodes as it minimizes the concentration decay. To sum up, the lower the concentration decay along the main propagation paths originated in s, the lower d_{sr}, the higher the closeness centrality of s ($C_{\mathrm{clos},s}$). From this definition, the metric seems to capture the physics of the process well. But the farthest nodes from s have the longest shortest paths (d_{sr} is even ∞ for the unconnected couples of nodes) and thus the highest influence in the estimation of $C_{\mathrm{clos},s}$. Conversely, in the physical process, the farthest spots are hardly reached by the propagation plume and therefore do not contribute to the danger associated with the source. To overcome this issue, we use the harmonic mean of the shortest paths by introducing the harmonic centrality [42,43]: $C_{\mathrm{harm},s} = \sum_{r\in\mathcal{V}} 1/d_{sr}$. In this way, the more node r is far from s, the longer the expected d_{sr}, and the less its contribution to $C_{\mathrm{harm},s}$. With this formulation, harmonic centrality takes into account the progressive concentration decay with distance from the source but still considers all the network nodes as affected by the spreading process. Conversely, the plume concentration along the shortest path becomes negligible at a certain point, and the most distant nodes, despite being connected, should not be considered in the centrality estimation of the source. For this reason, we propose the metric C_s as a tailored harmonic centrality with threshold on shortest path:

$$C_s = \sum_{r\in\mathcal{R}} \frac{1}{d_{sr}}, \tag{5}$$

with $r \in \mathcal{R}$ if

$$\frac{c_r}{c_s} = \prod_{(i,j)\in D} \frac{1}{w_{ij}} > \frac{c_{\mathrm{th}}}{c_0}, \tag{6}$$

where $c_s = c_0$ is the source concentration, c_r is the concentration at the target node, and c_{th} is the predefined threshold concentration. Condition (6) follows from the physical model proposed above [see Eq. (2) and the assumptions for propagation in the intersections], and it states that if the concentration along the shortest path between s and r ($\mathcal{D}$) falls below c_{th}, then r is excluded from the sum in Eq. (5). By means of the Heaviside function (Θ), Eqs. (5) and (6) can be rewritten together as

$$C_s = \sum_{r\in\mathcal{V}} \Theta\left[\prod_{(i,j)\in D} \frac{1}{w_{ij}} - \frac{c_{\mathrm{th}}}{c_0} \right] \frac{1}{d_{sr}}. \tag{7}$$

V. VULNERABILITY OF URBAN NETWORKS AND METRIC VALIDATION

By the proposed perspective, the spreading potential of a spot in a city is given by its centrality as a node in a flow network. Since the best spreading locations are here considered the most dangerous ones, vulnerability maps of urban areas are obtained in a straightforward manner as centrality maps. In Fig. 3 the vulnerability of an urban district in Lyon (France) is assessed for different wind directions. The study area is confined by physical boundaries (e.g., rivers, parks, railways) which act as discontinuity elements in the dispersion process and therefore justify the network delimitation. The nature of street interconnections and the distribution of link weights

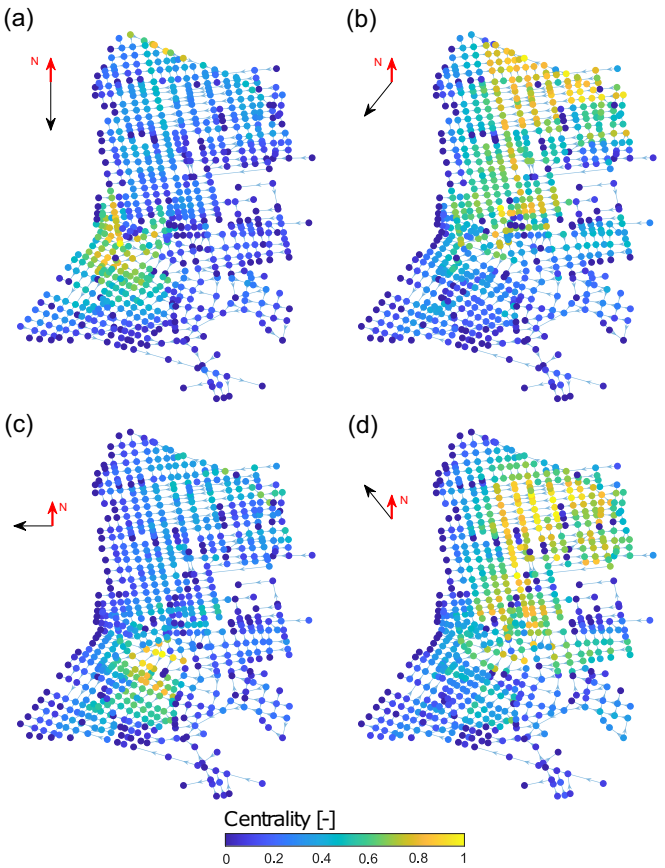

FIG. 3. Vulnerability maps in terms of spreading potential centrality for an urban district in Lyon for different wind directions: $\Phi = 0^\circ$ (a), 45° (b), 90° (c), and 135° (d). For each scenario, the centrality is normalized by its maximum value in the network.

(see Fig. 2) generate a strong heterogeneity in vulnerability, with marked differences even between neighboring nodes, and with a nontrivial location of the most vulnerable areas, the clusters of yellow (light gray) nodes. Moreover, the position of the critical nodes completely changes with the orientation of the wind. Figure 4 provides evidence for how different urban topologies exhibit distinctive behaviors to toxic emissions in the same meteorological scenario. The medieval structure of the city center in Florence (Italy) [Fig. 4(b)] has a sheltering effect to gas dispersion compared to the regular plan in Lyon.

To assess the validity of the proposed metric, we compare the centrality C_s of a node to the extent of its zone of influence (ZoI), i.e., the total length of the streets contaminated with a concentration above c_{th}, when the release takes place in the node. For each source location, this zone can be delimited using the algorithm proposed in Ref. [13]. In comparing the two approaches, we wonder whether a centrality metric based solely on shortest paths can capture the dispersion potential of a node given in terms of its total contaminated area. From a computational point of view, our centrality-based model brings clear advantages. In fact, existing and constantly improving algorithms developed in the field of complex network theory can be exploited to select the shortest paths and compute C_s.

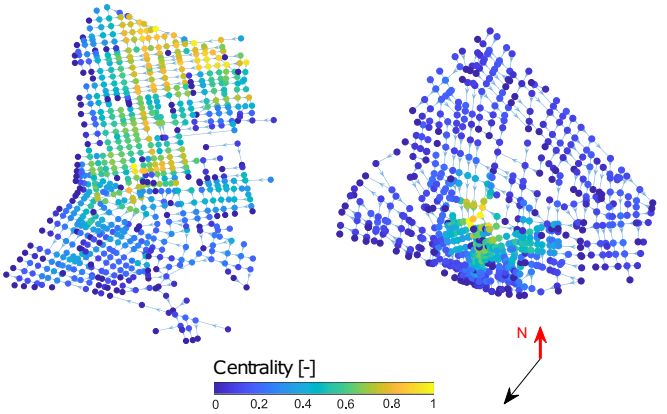

FIG. 4. Vulnerability maps in terms of spreading potential centrality for an urban district in Lyon (a) and Florence (b) for $\Phi = 45^\circ$. For each city, the centrality is normalized by its maximum value in the network.

In Fig. 5 the node ranking based on C_s is compared to the one obtained from the extent of the zone of influence. For the urban districts of Lyon, scenarios with two distinct initial concentrations ($c_0/c_{\text{th}} = 10$ and 100) are assessed. In each panel, the results for eight different wind directions are reported together. The high correlation in terms of coefficient of determination R^2 (>0.94) reveals a satisfactorily estimate of the spreading potential of a source node. In Table I the same correlation index is reported for the standard distance centrality metrics considered above (for the sake of conciseness we show only results about the $c_0/c_{\text{th}} = 10$ scenario). Adopting the fluid-dynamic weight expressed in Eq. (3) and analyzing the metrics in the same order followed for the definition of the new centrality C_s [Eq. (7)], we observe a progressive increase in R^2. Although the performance of harmonic centrality is good in terms of R^2 ($R^2 = 0.82$), the proposed centrality metric provides much more reliable results for applications.

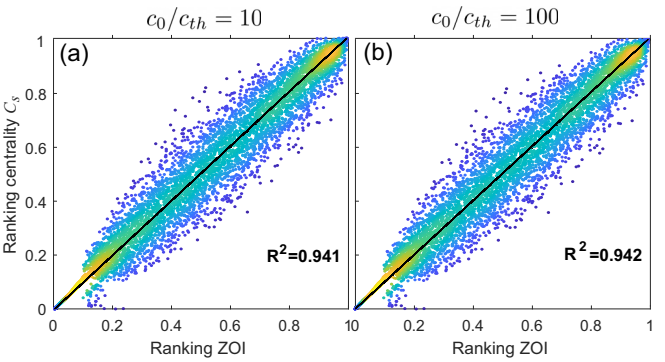

FIG. 5. Ranking of centrality C_s vs ranking of the extent of the zone of influence for $c_0/c_{\text{th}} = 10$ (left column) and $c_0/c_{\text{th}} = 100$ (left column) for the city of Lyon. The points correspond to the network nodes in multiple wind direction scenarios: $\Phi = 0^\circ$, 45°, 90°, 135°, 180°, 225°, 270°, 315°. The color (grayscale intensity) of the nodes is related to point density.

TABLE I. Results in terms of R^2 for the comparison between the ranking of the zone of influence and the ranking of different centrality metrics. As in Fig. 5(a), the scenarios with $c_0/c_{\text{th}} = 10$ in a district of Lyon are considered.

Centrality	R^2
Betweenness	0.26
Closeness	0.54
Harmonic	0.82
Spreading centrality C_s [Eq. (7)]	0.94

VI. CONCLUSIONS

To summarize, in this work we made a parallel between the atmosphere in the urban canopy layer and a flow network. In this way, pollutant dispersion from a point source was modeled as an epidemic on a complex network. Reviewing the previous literature, we evidenced the need for a centrality metric tailored to mass dispersion. Following a physical-based rationale, we proposed a centrality metric, and we assessed its effectiveness in the estimate of the spreading potential of a node. Within this innovative perspective, vulnerability maps of urban districts are easily traced for multiple scenarios, the critical areas are identified, and the structural fragility of a city is investigated.

These results demonstrate that the formal description of a physical phenomenon in terms of networks brings significant benefits from both a conceptual and computational point of view. This research paves the way for fascinating studies on the role of urban topology on the dispersion of airborne pollutants and the use of the proposed centrality for describing confined (e.g., due to decay processes) spreading phenomena.

[1] B. Brunekreef and S. T. Holgate, Air pollution and health, Lancet **360**, 1233 (2002).

[2] J. Coaffee, C. Moore, D. Fletcher, and L. Bosher, Resilient design for community safety and terror-resistant cities, P. I. Civil Eng.-Munic. **161**, 103 (2008).

[3] L. Soulhac, P. Salizzoni, F.-X. Cierco, and R. Perkins, The model SIRANE for atmospheric urban pollutant dispersion; part I, presentation of the model, Atmos. Environ. **45**, 7379 (2011).

[4] Y. Tominaga and T. Stathopoulos, CFD modeling of pollution dispersion in building array: Evaluation of turbulent scalar flux modeling in RANS model using LES results, J. Wind Eng. Ind. Aerod. **104**, 484 (2012).

[5] L. Soulhac, P. Salizzoni, P. Mejean, and R. Perkins, Parametric laws to model urban pollutant dispersion with a street network approach, Atmos. Environ. **67**, 229 (2013).

[6] S. Di Sabatino, R. Buccolieri, and P. Salizzoni, Recent advancements in numerical modelling of flow and dispersion in urban areas: A short review, Int. J. Environ. Poll. **52**, 172 (2013).

[7] R. Guimera, S. Mossa, A. Turtschi, and L. N. Amaral, The worldwide air transportation network: Anomalous centrality, community structure, and cities' global roles, Proc. Natl. Acad. Sci. USA **102**, 7794 (2005).

[8] R. Carvalho, L. Buzna, F. Bono, E. Gutiérrez, W. Just, and D. Arrowsmith, Robustness of trans-European gas networks, Phys. Rev. E **80**, 016106 (2009).

[9] S. P. Borgatti, A. Mehra, D. J. Brass, and G. Labianca, Network analysis in the social sciences, Science **323**, 892 (2009).

[10] M. Gelbrecht, N. Boers, and J. Kurths, A complex network representation of wind flows, Chaos **27**, 035808 (2017).

[11] E. Ser-Giacomi, R. Vasile, E. Hernández-García, and C. López, Most probable paths in temporal weighted networks: An application to ocean transport, Phys. Rev. E **92**, 012818 (2015).

[12] G. Iacobello, S. Scarsoglio, J. G. M. Kuerten, and L. Ridolfi, Spatial characterization of turbulent channel flow via complex networks, Phys. Rev. E **98**, 013107 (2018).

[13] S. Fellini, P. Salizzoni, L. Soulhac, and L. Ridolfi, Propagation of toxic substances in the urban atmosphere: A complex network perspective, Atmos. Environ. **198**, 291 (2019).

[14] S. Boccaletti, V. Latora, Y. Moreno, M. Chavez, and D.-U. Hwang, Complex networks: Structure and dynamics, Phys. Rep. **424**, 175 (2006).

[15] A. Barrat, M. Barthelemy, and A. Vespignani, *Dynamical Processes on Complex Networks* (Cambridge University Press, New York, 2008).

[16] M. E. J. Newman, Spread of epidemic disease on networks, Phys. Rev. E **66**, 016128 (2002).

[17] C. H. Comin and L. da Fontoura Costa, Identifying the starting point of a spreading process in complex networks, Phys. Rev. E **84**, 056105 (2011).

[18] R. Pastor-Satorras and A. Vespignani, Epidemic spreading in scale-free networks, Phys. Rev. Lett. **86**, 3200 (2001).

[19] M. Kitsak, L. K. Gallos, S. Havlin, F. Liljeros, L. Muchnik, H. E. Stanley, and H. A. Makse, Identification of influential spreaders in complex networks, Nat. Phys. **6**, 888 (2010).

[20] P. Basaras, D. Katsaros, and L. Tassiulas, Detecting influential spreaders in complex, dynamic networks, Computer **46**, 24 (2013).

[21] R. M. May and A. L. Lloyd, Infection dynamics on scale-free networks, Phys. Rev. E **64**, 066112 (2001).

[22] L. Soulhac and P. Salizzoni, Dispersion in a street canyon for a wind direction parallel to the street axis, J. Wind Eng. Ind. Aerod. **98**, 903 (2010).

[23] L. Soulhac, R. J. Perkins, and P. Salizzoni, Flow in a street canyon for any external wind direction, Bound.-Layer Meteorol. **126**, 365 (2008).

[24] P. Salizzoni, L. Soulhac, and P. Mejean, Street canyon ventilation and atmospheric turbulence, Atmos. Environ. **43**, 5056 (2009).

[25] L. Soulhac, V. Garbero, P. Salizzoni, P. Mejean, and R. Perkins, Flow and dispersion in street intersections, Atmos. Environ. **43**, 2981 (2009).

[26] P. Crucitti, V. Latora, and S. Porta, Centrality in networks of urban streets, Chaos **16**, 015113 (2006).

[27] M. Barthélemy, Spatial networks, Phys. Rep. **499**, 1 (2011).

[28] R. Ahujia, T. L. Magnanti, and J. B. Orlin, *Network Flows: Theory, Algorithms and Applications* (Prentice-Hall, 1993).

[29] D. Brockmann and D. Helbing, The hidden geometry of complex, network-driven contagion phenomena, Science **342**, 1337 (2013).

[30] A. Zeng and C.-J. Zhang, Ranking spreaders by decomposing complex networks, Phys. Lett. **377**, 1031 (2013).

[31] Y. Du, C. Gao, X. Chen, Y. Hu, R. Sadiq, and Y. Deng, A new closeness centrality measure via effective distance in complex networks, Chaos **25**, 033112 (2015).

[32] P. Van Mieghem, K. Devriendt, and H. Cetinay, Pseudoinverse of the Laplacian and best spreader node in a network, Phys. Rev. E **96**, 032311 (2017).

[33] S. Ahajjam and H. Badir, Identification of influential spreaders in complex networks using hybridrank algorithm, Sci. Rep. **8**, 11932 (2018).

[34] Ş. Erkol, C. Castellano, and F. Radicchi, Systematic comparison between methods for the detection of influential spreaders in complex networks, Sci. Rep. **9**, 15095 (2019).

[35] O. Diekmann and J. A. P. Heesterbeek, *Mathematical Epidemiology of Infectious Diseases: Model Building, Analysis and Interpretation*, Wiley Series in Mathematical and Computational Biology (John Wiley & Sons, 2000), Vol. 5.

[36] I. Nåsell, Stochastic models of some endemic infections, Math. Biosci. **179**, 1 (2002).

[37] U. Brandes, *Network Analysis: Methodological Foundations*, Lecture Notes in Computer Science, Vol. 3418 (Springer Science & Business Media, 2005).

[38] L. C. Freeman, A set of measures of centrality based on betweenness, Sociometry **40**, 35 (1977).

[39] E. Ser-Giacomi, A. Baudena, V. Rossi, R. Vasile, C. Lopez, and E. Hernández-García, From network theory to dynamical systems and back: Lagrangian betweenness reveals bottlenecks in geophysical flows, arXiv:1910.04722 (2019).

[40] M. E. Newman, *Networks: An Introduction* (Oxford University Press, New York, 2010).

[41] M. E. J. Newman, Scientific collaboration networks. II. Shortest paths, weighted networks, and centrality, Phys. Rev. E **64**, 016132 (2001).

[42] M. Marchiori and V. Latora, Harmony in the small-world, Physica A **285**, 539 (2000).

[43] Y. Rochat, Closeness centrality extended to unconnected graphs: The harmonic centrality index, Tech. Rep. No. EPFL-CONF-200525, Zurich, Switzerland (2009).